

Interfacial Assemblies **Hot Paper**How to cite: *Angew. Chem. Int. Ed.* **2021**, *60*, 8694–8699

International Edition: doi.org/10.1002/anie.202016217

German Edition: doi.org/10.1002/ange.202016217

Visualizing Interfacial Jamming Using an Aggregation-Induced-Emission Molecular Reporter

Pei-Yang Gu⁺, Feng Zhou⁺, Ganhua Xie⁺, Paul Y. Kim, Yu Chai, Qin Hu, Shaowei Shi, Qing-Feng Xu, Feng Liu, Jian-Mei Lu,^{*} and Thomas P. Russell^{*}

Abstract: With the interfacial jamming of nanoparticles (NPs), a load-bearing network of NPs forms as the areal density of NPs increases, converting the assembly from a liquid-like into a solid-like assembly. Unlike vitrification, the lineal packing of the NPs in the network is denser, while the remaining NPs can remain in a liquid-like state. It is a challenge to determine the point at which the assemblies jam, since both jamming and vitrification lead to a solid-like behavior of the assemblies. Herein, we show a real-time fluorescence imaging method to probe the evolution of the interfacial dynamics of NP surfactants at the water/oil interface using aggregation-induced emission (AIE) as a reporter for the transition of the assemblies into the jammed state. The AIEgens show typical fluorescence behavior at densities at which they can move and rotate. However, when aggregation of these fluorophores occurs, the smaller intermolecular separation distance arrests rotation, and a significant enhancement in the fluorescence intensity occurs.

The assembly of functional materials at liquid/liquid interfaces promises new opportunities in designing reconfigurable smart materials that are responsive to external stimuli.^[1] Nanoparticles (NPs) have been widely used to stabilize emulsions such as Pickering Emulsions. Recent studies have shown that functionalized NPs, dispersed in water, can assemble at the interface with a hydrophobic organic solution, containing ligands with complementary functionality, to form NP surfactants (NPSs).^[2] With NPSs, the ligands anchor to the NPs, markedly increasing the binding energy of the NPs to the interface, such that, when compressed, the NPS assembly will

jam at the interface.^[3] This jamming can then be used to lock-in non-equilibrium shapes of the aqueous phase.^[4] The jamming process, key to the structuring of liquids, occurs as the shape of the liquid phase changes to minimize the interfacial energy, increasing the areal density of the NPSs, leading to a jamming of the NPSs where a percolated pathway of NPSs forms that can support a load.^[5] Unlike vitrification, with jamming motion of the NPSs are arrested. While we understand the mechanism underlying the structuring of liquids, developing a means to isolate and monitor the point at which jamming occurs, that is, the point at which shape changes to the liquids be locked-in, are essential for the molding or three-dimensional (3D) printing of one liquid in another and to the development of all-liquid devices.^[6] There are no prior reports on the direct visualization of jamming at liquid–liquid interfaces. For systems absent liquids, TEM tomography is possible, but is time-intensive, and real-time measurements are not possible. For colloidal system, laser scanning confocal microscopy is possible, but isolating the specific colloids involved in the jamming process is not possible. For 2D assemblies, scanning probe microscopy is possible on static assemblies, but due to the scanning time and image analysis time, real-time measurements, in situ are not possible. Consequently, the method of fluorescence imaging based on aggregation induced emission (AIE) molecules fills a gap. The system self-selects the elements involved in the jamming and, hence, in providing the excess fluorescence emission and the massive increase in the fluorescence intensity characteristic of AIEgens provides the sensitivity

[*] Dr. P.-Y. Gu,^[†] Dr. F. Zhou,^[†] Prof. Q.-F. Xu, Prof. J.-M. Lu
College of Chemistry, Chemical Engineering and Materials Science
Collaborative Innovation Center of Suzhou Nano Science and
Technology, Soochow University
Suzhou 215123 (China)
E-mail: lujm@suda.edu.cn

Dr. P.-Y. Gu,^[†] Dr. G. Xie,^[†] Dr. P. Y. Kim, Dr. Q. Hu, Prof. T. P. Russell
Materials Sciences Division, Lawrence Berkeley National Laboratory
1 Cyclotron Road, Berkeley, CA 94720 (USA)

Dr. Y. Chai
Department of Physics, City University of Hong Kong
Kowloon (China)

Dr. Q. Hu
School of Microelectronics
University of Science and Technology of China
Hefei, Anhui 230026 (China)

Dr. F. Liu
Department of Physics and Astronomy, Collaborative Innovation
Center of IFSA (CICIFSA), Shanghai Jiaotong University
Shanghai 200240 (P. R. China)

Dr. Q. Hu, Prof. T. P. Russell
Polymer Science and Engineering Department
University of Massachusetts
Amherst, MA 01003 (USA)
E-mail: russell@mail.pse.umass.edu

Dr. S. Shi, Prof. T. P. Russell
Beijing Advanced Innovation Center for Soft Matter Science and
Engineering, Beijing University of Chemical Technology
Beijing 100029 (China)

Prof. T. P. Russell
Advanced Institute for Materials Research (WPI-AIMR)
Tohoku University
2-1-1 Katahira, Aoba, Sendai 980-8577 (Japan)

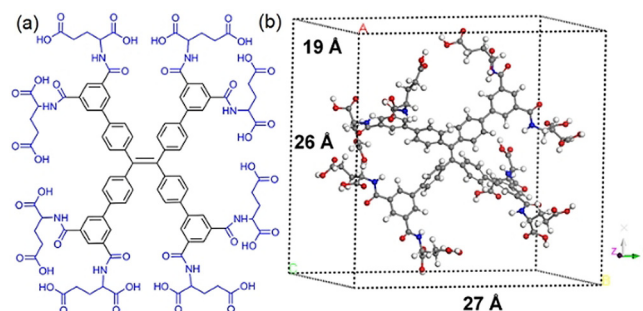
[†] These authors contributed equally to this work.

Supporting information and the ORCID identification number(s) for the author(s) of this article can be found under:
 <https://doi.org/10.1002/anie.202016217>.

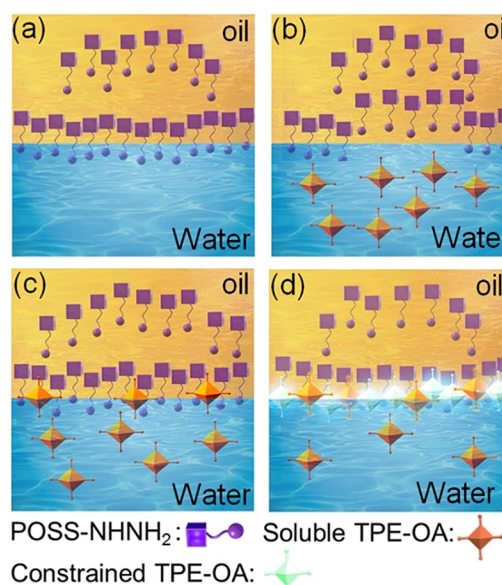
needed for a molecular reporting of some, but not all, of the chromophores assembled at the interface. In addition, the measurements are simple, can be done in situ and in real time, and the signal arises only from those AIEgens that are jammed.

A unique route by which the state of interfacial aggregation can be independently addressed is by use of AIE, a term introduced and popularized by Tang et al.^[7] Numerous AIEgens with tetraphenylethene (TPE) as a building block have been developed to harness their responsive optical properties.^[8] If we use a water soluble TPE-based derivative functionalized with carboxylic acid units that is dispersed in water as a functionalized NP, then, in contact with an oil, in which amine-functionalized ligands are dissolved, the electrostatic interactions between the TPE-based AIEgens and the ligands result in the formation of NPSs, significantly increasing the binding energy of the AIEgens at the interface. In solution, the phenyl rings of the TPE-based AIEgen derivative can rotate freely, dissipating energy upon excitation by thermal decay, quenching fluorescence.^[9] If the assemblies of AIEgens at an interface are liquid-like, a similar quenching occurs and only the inherent fluorescence of the AIEgen is seen. However, when the areal density of the interfacial assembly of the NPSs containing the TPE-based AIEgen derivative and ligand increases, as the system drives to reduce the interfacial area or interfacial energy, the separation distance between the NPSs decreases until the assembly jams, arresting a further decrease in the interfacial area, locking in the shape of the liquid. At the point of jamming, the interfacial assembly is a 2D aggregate and the interactions between adjacent TPE-based AIEgen surfactants restrict the motion of the phenyl rings and promote energy dissipation by emission, dramatically increasing the fluorescence. This can easily be detected by fluorescence microscopy, providing a molecular reporter of interfacial jamming.

Here, we demonstrate a real-time fluorescence imaging of the formation, assembly and dynamics of NPSs at the water/oil interface as the AIEgens undergo a transition from a liquid-like packing at the interface with a characteristic fluorescence intensity that reaches a maximum value as an increasing number of NPSs assemble at the interface, to an increased fluorescence level when a percolated pathway of the jammed NPSs exhibit AIE. For this study, a water-soluble nanometer-size TPE derivative, 2,2',2'',2''',2''''-((4',4''',4''''',4''''''-(ethene-1,1,2,2-tetrayl)tetrakis([1,1'-biphenyl]-3,5-dicarbonyl))octakis(azanediyl))octaglutaric acid (referred to as TPE-OA, Scheme 1), containing 16 carboxylic acid groups, was designed and synthesized. As shown in Scheme 2c, TPE-OA-based AIEgen surfactants can be formed in situ at the water/oil interface by electrostatic interactions between TPE-OA and aminoethylaminopropyl isobutyl polyhedral oligomeric silsesquioxane (referred to as POSS-NHNH₂, chemical structure shown in Scheme S1) dissolved in an oil phase. Without the amine functionalized ligands in the oil phase, the AIEgen will not assemble at the interface but, rather, are repelled from the inherently negatively charged water/oil interface.^[10] POSS-NHNH₂ shows strong interfacial activity, significantly reducing the interfacial tension, acting as a surfactant, and assembles at the



Scheme 1. a) Chemical structure of the functionalized TPE-OA lumogen used in this study, and b) DFT molecular simulation structure of the TPE-OA showing the dimensions of the molecule.



Scheme 2. a) Assembly of POSS-NHNH₂ at the oil/water interface. b) The TPE-OA-based AIEgen diffuses to the interface. c) Formation of NPSs between TPE-OA and POSS-NHNH₂ with a low amount of TPE-OA at the interface, causing an increase in fluorescence due to increased local concentration. d) AIE as the TPE-OA lumogens at the interface come into close enough contact to stimulate emission.

oil/water interface, as shown in Scheme 2a. The TPE-OA-based AIEgen then diffuses to the interface and interacts with the POSS-NHNH₂ to form the NPSs (Scheme 2b,c). As the interfacial area decreases to reduce the interfacial energy, the TPE-OA-based surfactants can either detach from the interface or remain at the interface depending on the binding energy. When the binding energy is too small, the TPE-OA-based lumogen will be ejected from the interface under compression, causing the fluorescence from the interface to have a value characteristic of a monolayer at the interface, and the liquid assumes a spherical shape, the shape with the smallest interfacial area for a given volume. As the binding energy increases, the TPE-OA-based lumogens are held at the interface under compression, the areal packing density increases to the point where a percolated pathway of NPSs forms that can support a load, that is, the NPSs jam, and an increase in the fluorescence is seen as the AIE occurs for the

jammed NPSs, as schematized in Scheme 2 d. The interfacial assemblies of the TPE-OA-based surfactants (NPSs) was investigated by the wrinkling of droplets under compression, in situ atomic force microscopy (AFM), the printing of all-liquids 3D structures, and laser scanning fluorescence confocal microscopy (LSFCM).

The synthesis of TPE-OA is shown in the supporting information (SI). To build a water-soluble nanometer-size TPE-cored AIEgen, a key intermediate, TPE-1, was synthesized by the Suzuki reaction between the phenyl group having two methoxycarbonyl end-capping substituents, and 1,1,2,2-tetrakis(4-bromophenyl)ethane. To increase the negative charges, TPE-1 was modified with a dendritic ligand by sequential hydrolysis, amidation, and hydrolysis reactions to produce TPE-OA having 16 carboxylic acid groups. The negative charges on the outer layer of TPE-OA increase the solubility of TPE-OA in water and prevents its aggregation. The detailed procedures and characterization data are given in SI. The size of the TPE-OA is $1.9 \times 2.6 \times 2.7 \text{ nm}^3$, as shown in Scheme 1 b.

The pH-dependence of the fluorescence was measured to understand the influence of TPE-OA ionization in water on aggregation. Figure 1 a shows a series of TPE-OA solutions in water as a function of pH and, in Figure 1 b, the corresponding fluorescence emission spectra. At a pH of 3.66, the TPE-OA solution emits strongly in the blue at a wavelength of maximum emission of $\lambda_{\text{max}} \approx 484 \text{ nm}$. When the pH is increased to approximately 5.44, the photoluminescence (PL) intensity dramatically decreases and shifts to the red, with a peak wavelength of $\lambda_{\text{max}} \approx 514 \text{ nm}$. This change in the fluorescence results from the deprotonation of TPE-OA to form negative ions and increasing its solubility in water. With the increased solubility, the intense AIE fluorescence is lost due to the increase in the separation distance between the AIEgens and increased intramolecular rotations. The PL intensity decreases slightly with a further increase in the pH value. AIE properties and fluorescence quantum yield of TPE-OA were further investigated in Figures S3–S5.

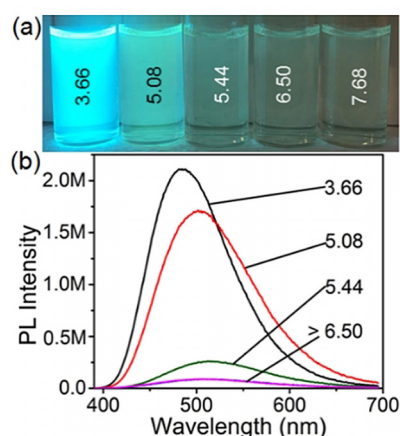


Figure 1. a) Photographs of TPE-OA (0.1 g L^{-1}) in aqueous solutions at different pH values under 365 nm UV illumination. b) Fluorescence spectra of TPE-OA (0.1 g L^{-1}) in aqueous solutions at different pH values ($\lambda_{\text{ex}} = 350 \text{ nm}$).

The dependence of the interfacial tension (γ) on pH was measured using pendant drop tensiometry with droplets of aqueous TPE-OA solutions suspended in silicone oil solutions of POSS-NH₂. For the pure water and pure silicone oil interface, γ is approximately 42.0 mN m^{-1} , as shown in Figure S6. With only TPE-OA (0.1 g L^{-1} , pH 5.44), γ is approximately 40.7 mN m^{-1} , indicating essentially no interfacial activity of TPE-OA at this pH, due to the inherent negative charge of the water/silicone oil interface.^[10] With only POSS-NH₂ (0.01 g L^{-1}), γ decreases to approximately 30.0 mN m^{-1} , indicating that POSS-NH₂+NH₃⁺ behaves like a surfactant, segregating to the water/silicone oil interface. At a pH of 7.68 for POSS-NH₂ (0.005 g L^{-1}) in silicone oil against TPE-OA (0.1 g L^{-1}) in water, γ gradually decreases to approximately 37.5 mN m^{-1} after 2100 s and then decreases more rapidly to 30.8 mN m^{-1} after about 2400 s (Figure 2 a). Similar behavior is seen with decreasing pH with the distinct difference that, with decreasing pH, the point at which the rapid drop in γ occurs shifts to shorter times of approximately 1800, 1500 and 1000 s for pH values of 6.5, 5.44 and 5.08, respectively. With a further decrease in the pH to 3.66, γ decreases very rapidly to about 36 mN m^{-1} and then gradually decreases to approximately 30 mN m^{-1} after 1300 s and then begins to decrease more rapidly. These time evolutions of γ reflect the electrostatic interactions between POSS-NH₂ and TPE-OA at the water/oil interface and the strength of these interactions. With decreasing pH value the degree of protonation of the POSS-NH₂ to POSS-NH₂⁺+NH₃⁺ increases, increasing its interfacial activity, leading to the initial gradual decrease in γ . With the increasing degree of protonation, come the increase in the electrostatic interactions with the TPE-OA to form essentially a TPE-OA: POSS-

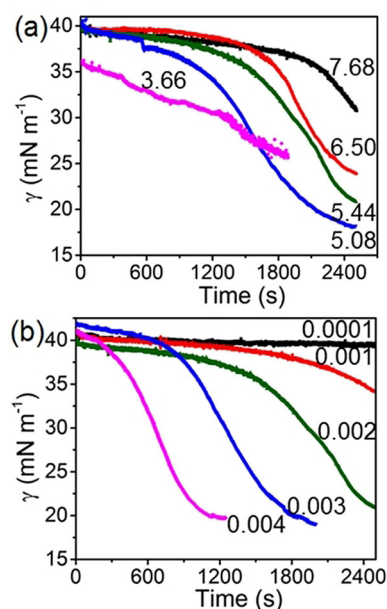


Figure 2. a) The pH-dependent interfacial assembly of TPE-OA (0.1 g L^{-1}) in water against POSS-NH₂ (0.002 g L^{-1}) in silicone oil. b) Time-evolution of the interfacial tension of TPE-OA (0.1 g L^{-1} , pH 5.44) in water against POSS-NH₂ in silicone oil at different concentrations (g L^{-1}).

$\text{NH}_2^+\text{NH}_3^+$ surfactant with an increased interfacial binding energy, as evidenced by the ability of these assemblies to wrinkle upon compression, as discussed later. At a pH of 3.66, the TPE-OA, as evidenced from the fluorescence, should aggregate in the water phase to form an AIEgen and it is AIEgen that interacts with the $\text{POSS-NH}_2^+\text{NH}_3^+$ assembled at the interface. Since these entities are larger, effectively NPs, they will affect a larger reduction in γ initially, since multiple $\text{POSS-NH}_2^+\text{NH}_3^+$ will interact with one of these aggregates, forming NPSs, with even higher binding energies. It is apparent that the assembly dynamics changes when the pH decreases to a point where the TPE-OA can aggregate. Figure 2b shows the time evolution of γ with TPE-OA in the water solution and POSS-NHNH_2 in the silicone oil solution at a pH of 5.44, where the concentration of POSS-NHNH_2 was varied. γ decreases with increasing POSS-NHNH_2 concentration. At the lowest POSS-NHNH_2 concentration (0.0001 g L^{-1}), γ decreases slightly to 39.5 mN m^{-1} and remains relatively constant, due to the low concentration of $\text{POSS-NH}_2^+\text{NH}_3^+$ at the interface. As the concentration of POSS-NHNH_2 is increased, clear evidence is seen for the increased segregation of $\text{POSS-NH}_2^+\text{NH}_3^+$ to the interface by the initial increased rate of reduction in γ and then, the increased interactions between $\text{POSS-NH}_2^+\text{NH}_3^+$ and TPE-OA, as evidenced by the more rapid decrease in γ after approximately 2000, 1800, 800 and 500 s for POSS-NHNH_2 concentrations of 0.001, 0.002, 0.003 and 0.004 g L^{-1} , respectively. This reflects the availability of $\text{POSS-NH}_2^+\text{NH}_3^+$ at the interface to interact with the TPE-OA to form a NPSs. For POSS-NHNH_2 concentrations of 0.003 g L^{-1} or higher, the interactions between the TPE-OA^{16-} and $\text{POSS-NH}_2^+\text{NH}_3^+$ are so strong that a self-wrinkling of the assembly on the surface of the droplet is evident (Figure S8). The only way that this self-wrinkling can occur is that, after the surface of the droplet is saturated, additional TPE-OA-based AIEgen surfactants form and assemble at the interface, crowding the already saturated interface, forcing an out-of-plane deformation of the assembly, that is, wrinkling and buckling of the assembly since the surface area of the drop is fixed. The ratio of the volume at which wrinkling is observed in comparison to the initial volume, V_w/V_i , serves as an approximate measure of the initial coverage of the interface. Figure S9 shows that the surface coverage increases with the increase time, reflecting the formation and assembly of the TPE-OA-based AIEgen surfactants over time. The self-wrinkling behavior of the assemblies on the droplet surface was visualized using in situ AFM, as shown in Figures S11–S16, where the topography of the interfacial assembly reflects the wrinkling behavior.

We took advantage of the rapid TPE-OA-based AIEgen surfactant formation and assembly at the interface by printing liquid-in-liquid structures as shown in Figure 3a where a serpentine structure of TPE-OA (0.1 g L^{-1} , pH 6.50) was printed in a POSS-NHNH_2 (5.0 g L^{-1}) silicone oil (viscosity $60\,000 \text{ cSt}$) solution. A strong blue fluorescence under 365 nm UV illumination is evident due to the jamming of the TPE-OA-based AIEgen surfactants at the interface (Figure 3b). Absent POSS-NHNH_2 , TPE-OA-based AIEgen surfactants do not form, and only spherical domains with weak fluorescence are seen (Figure S17).

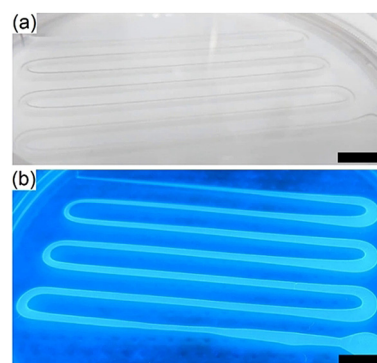


Figure 3. 3D-printed all-liquid systems. a) The sigmoidal structure was made by manual printing of TPE-OA (0.1 g L^{-1} , pH 6.50) in POSS-NHNH_2 (5.0 g L^{-1}) silicone oil (viscosity $60\,000 \text{ cSt}$) solution. Scale bar: 1 cm. b) Image of (a) under 365 nm UV illumination.

The formation and assembly of the TPE-OA-based AIEgen surfactants at the interface could be directly visualized by LSFCM. As shown in Figure 4a and Video S1, when a water droplet containing TPE-OA (0.1 g L^{-1} , pH 6.50) is placed in a solution of POSS-NHNH_2 (1.0 g L^{-1}) in silicone oil, the interface is difficult to see initially, due to the weak fluorescence of TPE-OA. After 10 min (Figure 4b), a weak fluorescence at the interface is observed, as $\text{POSS-NH}_2^+\text{NH}_3^+$ electrostatically interacts with TPE-OA^{16-} at the interface to form the NPSs. With increasing the time (Figure 4c–f), the fluorescence intensity at the interface increases. The fluorescence intensity appears to level off after about 60 min and then, begins to increase again and then decrease slightly. This is more evident when the time-dependence of the fluorescence intensity integrated over the interface is examined, as shown in Figure 4g. The fluorescence intensity increases as the TPE-OA interacts with the $\text{POSS-NH}_2^+\text{NH}_3^+$ assembled at the interface to form the NPSs up to a point where the interface is saturated. Here, the assemblies are still liquid-like and the fluorescence intensity only arises from the individual TPE-OA molecules that are located at the interface. Consequently, after 60 min, the interface saturates and the fluorescence intensity reaches a plateau. With increasing time, more TPE-OA can interact with the $\text{POSS-NH}_2^+\text{NH}_3^+$, due to the diffusive motions of the molecules assembled at the interface, leading to an in-plane crowding and jamming of the $\text{TPE-OA}:\text{POSS-NH}_2^+\text{NH}_3^+$. The percolated networks forced during the jamming forces a limited number of the TPE-OAs to be close enough to give rise to AIE and, hence an increase in the fluorescence intensity. If all the TPE-OAs were involved, a much greater increase in the fluorescence intensity would be observed.

The modest increase reflects only the $\text{TPE-OA}:\text{POSS-NH}_2^+\text{NH}_3^+$ involved in the jamming and, hence, reports on the jamming process. Since changes to the interfacial area are locked-in due to the jamming, the fluorescence intensity does not increase further but, rather, remains constant. With increasing time, some of the fluorescent molecules are photobleached and the fluorescence intensity begins to decrease (Figures S19 and S20). As shown in Figures 5 and S21 and Video S2, interfacial jamming can easily be detected

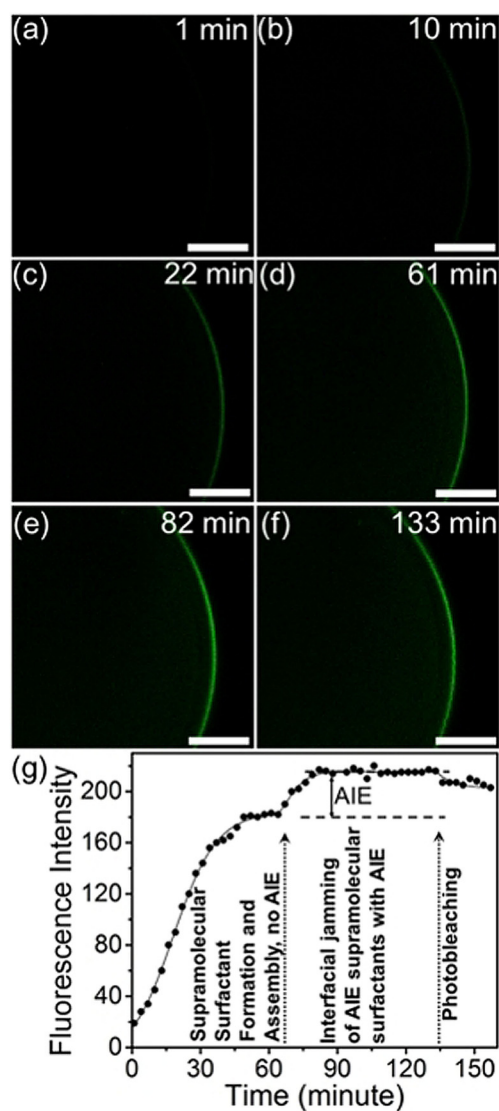


Figure 4. a–f) Confocal fluorescence microscopy images (at 1, 10, 22, 61, 82, 133 min; scale bar: 200 nm) and g) fluorescence intensity of water droplets containing TPE-OA (0.1 g L^{-1} , pH 6.50) surrounded by a silicone oil solution containing POSS-NH NH_2 (1.0 g L^{-1}) over time.

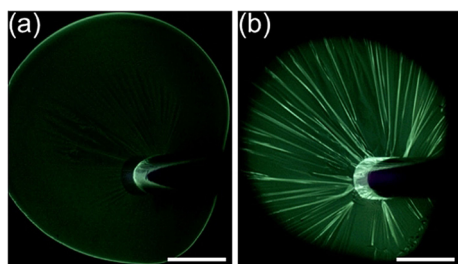


Figure 5. Optical images under 365 nm UV light of a water droplet containing TPE-OA (0.1 g L^{-1} , pH 6.50) surrounded by silicone oil solution containing POSS-NH NH_2 (1.0 g L^{-1}): a) aging for 30 min; b) decreasing the volume of the droplet. Scale bar: 200 nm.

by a marked increase in the fluorescence when the volume of a pendant drop is decreased by withdrawing the aqueous solution into the needle. As the volume decreases, interfacial

area decreases, causing the jammed assembly to wrinkle and fold. When the assembly wrinkles, no significant increase in the fluorescence intensity is seen. However, when the assembly buckles and folds, the AIEgens are forced closer together in the folds and a dramatic increase in the fluorescence intensity is seen in the folds, highlighting the folds in a very dramatic manner, even on the tip of the needle.

In conclusion, a molecular reporter for visualizing interfacial jamming based on an AIE platform has been developed. A water-soluble TPE derivative TPE-OA containing 16 carboxylic acid groups was designed and successfully synthesized, with AIE characteristics. TPE-OA-based AIEgen surfactants can be formed in situ at the water/oil interface through electrostatic interactions between TPE-OA and POSS-NH NH_2 . The formation and assembly of the AIEgen surfactants could be monitored in real time by γ and fluorescence intensity, with AIE serving as a reporter as to when jamming of the assemblies occurred. The PL intensity at the interface increases with increasing assembly time, indicating that increased formation and assembly of TPE-OA-based AIEgen surfactants. The binding energy of the NPSs is sufficiently high to withstand compressive forces, as evidenced by the wrinkling behavior observed during a reduction in the volume of the droplet. Consequently, the NPSs assemblies can jam and lock-in shape changes of the liquid phases. In comparison to conventional electron microscope imaging and fluorescence imaging based on traditional chromophores, the TPE-OA-based AIEgen NPS provide a unique means with highly sensitive and contrast to monitor interfacial assembly, and the interfacial jamming of the assemblies.

Acknowledgements

The interfacial assembly, jamming and chromogenic behavior were supported by the U.S. Department of Energy, Office of Science, Basic Energy Sciences under Contract No. DE-AC02-05-CH11231 within the Adaptive Interfacial Assemblies Towards Structuring Liquids program (KCTR16). The synthesis and spectroscopy were supported by the National Natural Science Foundation of China (21938006 and 51803143), the National Key Technology Research and Development Program (2020YFC1818401), and Basic Research Project of Leading Technology in Jiangsu Province (BK20202012).

Conflict of interest

The authors declare no conflict of interest.

Keywords: 3D printing · aggregation-induced emission · interfaces · interfacial jamming · structured liquids

- [1] a) Z. Yang, J. Wei, Y. I. Sobolev, B. A. Grzybowski, *Nature* **2018**, 553, 313–318; b) L. D. Zarzar, V. Sresht, E. M. Sletten, J. A. Kalow, D. Blankshtein, T. M. Swager, *Nature* **2015**, 518, 520–

- 524; c) Y. Zheng, Z. Yu, R. M. Parker, Y. Wu, C. Abell, O. A. Scherman, *Nat. Commun.* **2014**, *5*, 5772; d) Y. Chao, H. C. Shum, *Chem. Soc. Rev.* **2020**, *49*, 114–142; e) C. Buten, L. Kortekaas, B. J. Ravoo, *Adv. Mater.* **2020**, *32*, 1904957; f) R. T. Shafraanek, S. C. Millik, P. T. Smith, C.-U. Lee, A. J. Boydston, A. Nelson, *Prog. Polym. Sci.* **2019**, *93*, 36–67.
- [2] a) M. Cui, T. Emrick, T. P. Russell, *Science* **2013**, *342*, 460–463; b) R. Luo, J. Dong, X. Li, Y. Luo, *Colloid Polym. Sci.* **2020**, *298*, 419–433.
- [3] a) H. M. Jaeger, *Soft Matter* **2015**, *11*, 12–27; b) C. Huang, J. Forth, W. Wang, K. Hong, G. S. Smith, B. A. Helms, T. P. Russell, *Nat. Nanotechnol.* **2017**, *12*, 1060–1063; c) P. Y. Gu, Y. Chai, H. Hou, G. Xie, Y. Jiang, Q. F. Xu, F. Liu, P. D. Ashby, J. M. Lu, T. P. Russell, *Angew. Chem. Int. Ed.* **2019**, *58*, 12112–12116; *Angew. Chem.* **2019**, *131*, 12240–12244.
- [4] a) Z. Niroobakhsh, J. A. LaNasa, A. Belmonte, R. J. Hickey, *Phys. Rev. Lett.* **2019**, *122*, 178003; b) X. Liu, N. Kent, A. Ceballos, R. Streubel, Y. Jiang, Y. Chai, P. Y. Kim, J. Forth, F. Hellman, S. Shi, *Science* **2019**, *365*, 264–267.
- [5] a) W. Feng, Y. Chai, J. Forth, P. D. Ashby, T. P. Russell, B. A. Helms, *Nat. Commun.* **2019**, *10*, 1095; b) G. Xie, J. Forth, Y. Chai, P. D. Ashby, B. A. Helms, T. P. Russell, *Chem* **2019**, *5*, 2678–2690; c) X. Hua, M. A. Bevan, J. Frechette, *Langmuir* **2018**, *34*, 4830–4842.
- [6] a) G. Luo, Y. Yu, Y. Yuan, X. Chen, Z. Liu, T. Kong, *Adv. Mater.* **2019**, *31*, 1904631; b) L. Tran, M. F. Haase, *Langmuir* **2019**, *35*, 8584–8602; c) J. Forth, X. Liu, J. Hasnain, A. Toor, K. Miszta, S. Shi, P. L. Geissler, T. Emrick, B. A. Helms, T. P. Russell, *Adv. Mater.* **2018**, *30*, 1707603.
- [7] J. Luo, Z. Xie, J. W. Lam, L. Cheng, H. Chen, C. Qiu, H. S. Kwok, X. Zhan, Y. Liu, D. Zhu, B. Z. Tang, *Chem. Commun.* **2001**, 1740–1741.
- [8] a) Z. Wei, Z. Y. Gu, R. K. Arvapally, Y. P. Chen, R. N. McDougald, Jr., J. F. Ivy, A. A. Yakovenko, D. Feng, M. A. Omary, H. C. Zhou, *J. Am. Chem. Soc.* **2014**, *136*, 8269–8276; b) W. Guan, S. Wang, C. Lu, B. Z. Tang, *Nat. Commun.* **2016**, *7*, 11811; c) Y. L. Ying, Y. J. Li, J. Mei, R. Gao, Y. X. Hu, Y. T. Long, H. Tian, *Nat. Commun.* **2018**, *9*, 3657.
- [9] a) W. Guan, W. Zhou, C. Lu, B. Z. Tang, *Angew. Chem. Int. Ed.* **2015**, *54*, 15160–15164; *Angew. Chem.* **2015**, *127*, 15375–15379; b) Z. Li, P. Liu, X. Ji, J. Gong, Y. Hu, W. Wu, X. Wang, H. Q. Peng, R. T. K. Kwok, J. W. Y. Lam, J. Lu, B. Z. Tang, *Adv. Mater.* **2020**, *32*, 1906493.
- [10] a) K. G. Marinova, R. G. Alargova, N. D. Denkov, O. D. Velev, D. N. Petsev, I. B. Ivanov, R. P. Borwankar, *Langmuir* **1996**, *12*, 2045–2051; b) J. K. Beattie, A. M. Djerdjev, *Angew. Chem. Int. Ed.* **2004**, *43*, 3568–3571; *Angew. Chem.* **2004**, *116*, 3652–3655; c) J. Stachurski, M. Michałek, *J. Colloid Interface Sci.* **1996**, *184*, 433–436; d) P. Creux, J. Lachaise, A. Graciaa, J. K. Beattie, A. M. Djerdjev, *J. Phys. Chem. B* **2009**, *113*, 14146–14150; e) D. E. Dunstan, *J. Colloid Interface Sci.* **1994**, *166*, 472–475.

Manuscript received: December 6, 2020

Accepted manuscript online: January 24, 2021

Version of record online: March 8, 2021